GEOLOGY | THE GEOLOGICAL SOCIETY OF AMERICA®

https://doi.org/10.1130/G51939.1

Manuscript received 4 December 2023
Revised manuscript received 1 April 2024
Manuscript accepted 15 April 2024

Published online 23 April 2024

Alkenone-derived estimates of Cretaceous pCO_2

Weimin Si[1,*], Joseph B. Novak[2], Nora Richter[3], Pratigya Polissar[2], Ruigang Ma[4,5], Ewerton Santos[1], Jared Nirenberg[1], Timothy D. Herbert[1], and Marie-Pierre Aubry[5]

[1]Department of Earth, Environmental and Planetary Sciences, Brown University, Providence, Rhode Island 02912, USA
[2]Ocean Sciences Department, University of California, Santa Cruz, California 95064, USA
[3]Department of Marine Microbiology and Biogeochemistry, Royal Netherlands Institute for Sea Research (NIOZ), 1790 AB Den Burg, Netherlands
[4]State Key Laboratory of Marine Geology, Tongji University, Shanghai 200092, China
[5]Department of Earth and Planetary Sciences, Rutgers University, New Brunswick, New Jersey 08854, USA

ABSTRACT

Alkenones are long-chain ketones produced by phytoplankton of the order Isochrysidales. They are widely used in reconstructing past sea surface temperatures, benefiting from their ubiquitous occurrence in the Cenozoic ocean. Carbon isotope fractionation (ε_p) between alkenones and dissolved inorganic carbon may also be used as a proxy for past atmospheric pCO_2 and has provided continuous pCO_2 estimates back to ca. 45 Ma. Here, an extended occurrence of alkenones from ca. 130 Ma is reported. We characterize the molecular structure and distribution of these Mesozoic alkenones and evaluate their potential phylogenetic relationship with Cenozoic alkenones. Using $\delta^{13}C$ values of the C_{37} methyl alkenone ($C_{37:2}Me$), the first alkenone-based pCO_2 estimates for the Mesozoic are derived. These estimates suggest elevated pCO_2 with a range of 548–4090 ppm (908 ppm median) during the super-greenhouse climate of the Early Cretaceous, in agreement with phytane-based pCO_2 reconstructions. Finally, insights into the identity of the Cretaceous coccolithophores that possibly synthesized alkenones are also offered.

INTRODUCTION

The Earth's climate has undergone a transition from a hothouse climate during the Cretaceous (ca. 143–66 Ma) and early Paleogene (66–33 Ma) to an icehouse climate in the late Cenozoic (Hay and Floegel, 2012). Sea surface temperature (SST) reconstructions using organic biomarkers and $\delta^{18}O$ of exceptionally well-preserved planktonic foraminifera confirm that the Cretaceous climate was hot with flattened meridional gradients (Pearson et al., 2001; O'Brien et al., 2017). Post-Cretaceous cooling was accompanied by a decline in atmospheric pCO_2; knowledge of Cretaceous CO_2 levels, however, remains limited ($CENCO_2PIP$ Consortium, 2023).

Based primarily on terrestrial leaf stomata, liverwort $\delta^{13}C$, pedogenic carbonate $\delta^{13}C$, and nahcolite, estimates for atmospheric pCO_2 prior to 45 Ma range from 100 to 2000 ppm for the Cretaceous (Foster et al., 2017; Jagniecki et al., 2015). $\delta^{13}C$ of algae-derived phytane has also been used as a pCO_2 proxy (Witkowski et al., 2018), but fossil phytane is derived from a wide variety of marine algae with potentially different isotopic fractionations, complicating its application.

For the Cenozoic, marine proxies, including boron isotopes of planktonic foraminifera and $\delta^{13}C$ of alkenones, are widely used for pCO_2 estimates ($CENCO_2PIP$ Consortium, 2023). Marine alkenones are thought to have a restricted biological source, being mainly produced by species of the family Noëlaerhabdaceae in the order Isochrysidales (Marlowe et al., 1990; Henderiks and Pagani, 2008; Brassell, 2014). Efforts have also been made to take into account potential complicating factors such as growth rates and active CO_2 acquisition, allowing for more accurate alkenone-based paleo-pCO_2 reconstructions (Stoll et al., 2019). Alkenones, however, have not yet been used to estimate Cretaceous pCO_2 levels.

Here, we report the extended occurrence of alkenones from the Early and Late Cretaceous (ca. 80–130 Ma) in hemipelagic settings from the Atlantic Basin. Similar to their Cenozoic counterparts where continuous alkenone-based pCO_2 was estimated (Zhang et al., 2013), organic-rich hemipelagic Cretaceous sediments preserve abundant and diverse alkenones that allow us to characterize their molecular profiles, structures, and carbon isotopic compositions. From this, we derive the first Cretaceous pCO_2 estimates, highlighting the possibility of extending alkenone-based pCO_2 estimates from ca. 45 Ma to ca. 130 Ma. We also discuss the potential implications of identifying early alkenones for determining the origin of alkenone producers in the Cretaceous in combination with coccolith fossil evidence.

METHODS AND RESULTS

Cretaceous hemipelagic sediments from five North Atlantic Deep Sea Drilling Project (DSDP) and Ocean Drilling Program (ODP) sites were examined (Fig. 1). Total organic carbon content reached up to 10% in the studied sediments, indicating anoxic conditions that favor the preservation of organic matter. Analysis of alkenones and pCO_2 calculations are detailed in the Supplemental Material[1]. Sample ages were assessed using shipboard biostratigraphy (Table S1 in the Supplemental Material).

Gas chromatography–mass spectrometry analysis reveals a series of di-unsaturated alkenones (alkadienones) in samples from all five sites, with no alkatrienones (Fig. 1). The oldest samples, from ODP Site 638 (early Berriasian–middle Valanginian), contained four alkadienones: the C_{36} di-unsaturated ethyl

Weimin Si https://orcid.org/0000-0002-3835-3376
*weimin_si@brown.edu

[1]Supplemental Material. Sample chronology, detailed analytical and pCO_2 estimate methods, fossil taxon descriptions, supporting data tables, and supplementary figures showing alkenone distributions and mass spectra. Please visit https://doi.org/10.1130/GEOL.S.25611891 to access the supplemental material; contact editing@geosociety.org with any questions.

CITATION: Si, W., et al., 2024, Alkenone-derived estimates of Cretaceous pCO_2: Geology, v. XX, p. , https://doi.org/10.1130/G51939.1

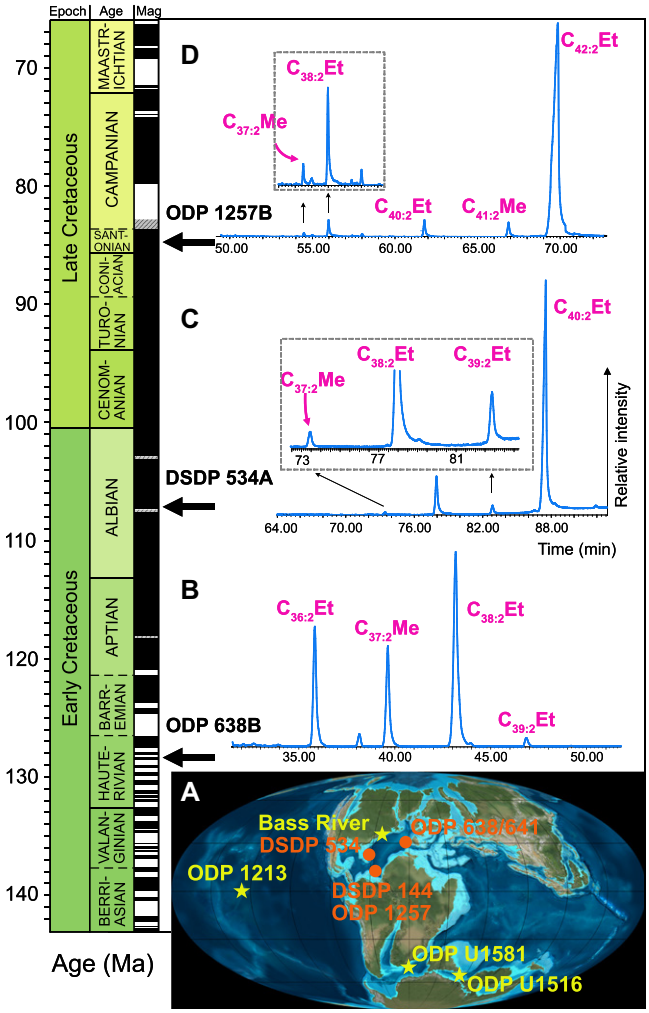

Figure 1. (A) Sample sites for this study and previous studies. DSDP—Deep Sea Drilling Project; ODP—Ocean Drilling Program. (B–D) Gas chromatograms of selected samples: ODP-638B-22-4-21 (B), DSDP-534A-29-1-70 (C), and ODP-1257B-19-1-100 (D). Note that the elution times are different among samples because we used different columns and gas chromatography methods (Table S2 [see text footnote 1]). Mag—magnetic reversal; Et—ethyl; Me—methyl. Yellow star in A indicates known Cretaceous alkenone (Brassell et al., 2004; de Bar et al., 2019; Doiron et al., 2023; Hasegawa and Goto, 2024). Early Cretaceous geography in A was created using TSCreator (https://timescalecreator.org).

(Et) ketone ($C_{36:2}$Et), C_{37} methyl (Me) ketone ($C_{37:2}$Me), $C_{38:2}$Et, and $C_{39:2}$Et (Fig. 1). Samples from DSDP Site 534 (mid-Albian) contained no $C_{36:2}$Et but yielded abundant $C_{38:2}$Et and $C_{40:2}$Et. In the youngest samples, from ODP Site 1257 (early Campanian), $C_{40:2}$Et, $C_{41:2}$Me, and $C_{42:2}$Et were abundant.

We identified a rare alkenone constituent of $C_{36:2}$Et in the ODP Site 638 samples (Fig. 2). This alkenone was previously observed in the early Aptian (Brassell et al., 2004). Dimethyl disulfide (DMDS) adducts and mass spectra suggest that this compound is a (12E, 21E)-hexatriaconta-12,21-dien-3-one where the positions of the carbon-carbon double bonds (Δ^{10} and Δ^{19}) are separated by nine carbons (C_9 separation) rather than the usual seven or five carbons (Figs. S2-A and S3-B in the Supplemental Material; Xu et al., 2001; Prahl et al., 2006). All other alkadienones identified in samples from ODP Site 638 have the conventional carbon-carbon double-bond positions: Δ^{14} and Δ^{21} (see Figs. S3–S5).

We have analyzed compound-specific $\delta^{13}C$ for $C_{36:2}$Et, $C_{37:2}$Me, $C_{38:2}$Et, $C_{39:2}$Et, and $C_{40:2}$Et alkenones in 12 samples (Table S8). Carbon isotope ratios are depleted in older samples (ODP Site 638, $C_{37:2}$Me, $-36‰ \pm 0.6‰$) and enriched in younger samples (ODP Site 1257, $C_{37:2}$Me, $-33.5‰ \pm 0.8‰$). The isotopic compositions of different alkenones are comparable, with a maximum difference of ~2.2‰ between $C_{36:2}$Et and $C_{38:2}$Et in the Hauterivian samples (ODP Site 638). Overall, our alkenone $\delta^{13}C$ values are in broad agreement with values reported from Ocean Anoxic Event 1 (120 Ma) in the Western Pacific ($C_{37:2}$Me, −31.3‰; $C_{38:2}$Et, −31.9‰) and Ocean Anoxic Event 2 in the Southern Ocean (92 Ma) ($C_{40:2}$Et, −33‰ to −29‰) (Brassell et al., 2004; Hasegawa and Goto, 2024).

We estimate the carbon isotope fractionation factor ε_p and pCO_2 using methods detailed in the Supplemental Material. The $\delta^{13}C$ of $C_{37:2}$Me (−31.6‰ and −37.2‰) suggests that the Cretaceous ε_p is in the range of 21.9‰–26.7‰ (Table S9). These are the most enriched values over the past 130 m.y. (Fig. 3).

DISCUSSION

Although alkenones are known from the Aptian (ca. 120 Ma) and younger intervals (Brassell et al., 2004; Dumitrescu and Brassell, 2005; de Bar et al., 2019; Doiron et al., 2023; Hasegawa and Goto, 2024), the temporal range, molecular structure, stable isotope signature, and candidate fossil producers of Cretaceous alkenones are yet to be fully explored, limiting their paleoclimatological potential. Here, we evaluate the potential of alkenones in our samples for reconstructing atmospheric pCO_2 concentrations.

The Cretaceous samples are characterized by the unique occurrence of $C_{36:2}$Et, $C_{40:2}$Et, $C_{41:2}$Me, and $C_{42:2}$Et alkenones (Fig. 1). These compounds are uncommon in Cenozoic marine sediments, although rare occurrences have been reported in modern and paleo-records from brackish waters (e.g., Black Sea, salinity ~17 PSU), saline lakes (Liao et al., 2020), and coastal settings (Yamamoto et al., 1996; Marlow et al., 2001). It has been suggested that these unusual alkenones were likely produced by brackish non-calcifying Isochrysidales belonging to Group II (Fig. 2C) (Huang et al., 2021).

The studied sites and other nearby drill sites are known for the preservation of middle to Late Cretaceous glassy planktonic foraminifera occurring in calcareous chalks interbedded with black shales (Fig. 1A; Table S5). Planktonic foraminifera are exclusively marine dwellers, sensitive to temperature, salinity, and hydrological changes. The co-occurrence of Cretaceous alkenones with planktonic foraminifera in the same geographic setting is thus strong evidence for the marine habitat of Cretaceous alkenone producers. Cretaceous alkenones were also observed in the central Pacific (Fig. 1A). The weight of the evidence is strongly against a brackish origin for the Cretaceous hemipelagic alkenones described here.

Further inspection of our Cretaceous alkenones reveals two unique features that are potentially related to their ancestral position. In the modern-day Black Sea, the double bonds of the $C_{36:2}$Et ketone occur at Δ^{14} and Δ^{19} (Xu et al., 2001), with a C_5 separation (Fig. 2A). In contrast, a cultured strain of *Emiliania huxleyi* (family Noëlaerhabdaceae, strain CCMP1742) produced a $C_{36:2}$Et ketone with double bonds occurring at Δ^{12} and Δ^{19} with the conventional C_7 separation (Fig. 2A) (Prahl et al., 2006). The double-bond positions of the newly identified Cretaceous $C_{36:2}$Et (Δ^{10} and Δ^{19}) are separated by nine carbons, which differs from both the Black Sea alkenones and the cultured *E. huxleyi* alkenones (Fig. 2A). Two biosynthetic pathways have been proposed for Cenozoic lineages that yield double bonds with a C_7 or C_5 separation (Rontani et al., 2006; Zheng et al., 2016); however, neither biosynthetic pathway nor proposed desaturases can account for the Δ^{10} double-bond position. In contrast to the persistent Δ^{14} and Δ^{21} double-bond positions in longer-chain alkenones, the biosynthetic pathway for short-chain $C_{36:2}$Et production appears to have undergone more changes throughout geologic history.

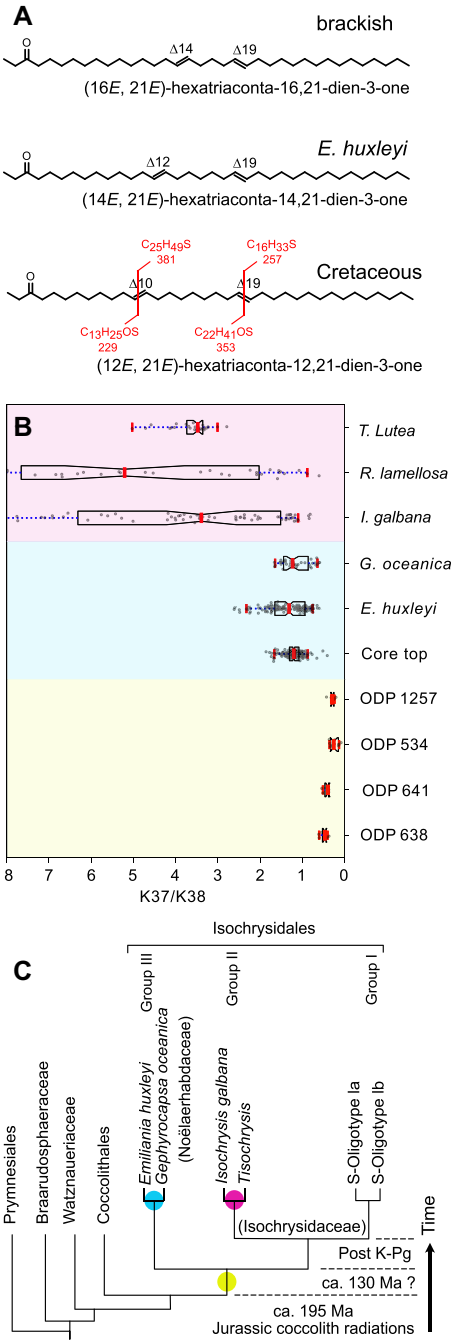

Figure 2. (A) Double-bond position of $C_{36:2}$Et in brackish (Isochrysidales Group II), marine Noëlaerhabdaceae (Isochrysidales Group III), and Cretaceous species, respectively. (B) Ratio of C_{37}:C_{38} alkenones, K37/K38, in three groups, as in A, respectively (Table S3 [see text footnote 1]). T—Tisochrysis; R—Ruttnera; I—Isochrysis; G—Gephyrocapsa; E—Emiliania; ODP—Ocean Drilling Program. (C) Molecular phylogeny of coccolithophores. Based on small-subunit ribosomal RNA, modern alkenone-producing haptophytes can be divided into three major groups: the more recently evolved Group I is found in freshwater lakes; its neighboring lineage, Group II, commonly occurs in brackish and estuary environments. All modern species of Isochrysidales share a last common ancestor dated to the Early Cretaceous (Medlin et al., 2008; Richter et al., 2019). Colors in B and C: yellow—Cretaceous alkenones; blue—Group III, marine Noëlaerhabdaceae; red—Group II (brackish Isochrysidales). K-Pg—Cretaceous-Paleogene boundary.

Another feature of our samples is the low ratio of C_{37} to C_{38} alkenones, K37/K38 (Fig. 2B). Modern Group II Isochrysidales, for instance, are characterized by large variability in the K37/K38 ratio (Table S3). In comparison, alkenones in globally distributed marine core-top samples have a typical K37/K38 ratio closer to 1, as do cultures of *E. huxleyi* and *Gephyrocapsa oceanica* (i.e., modern-day marine alkenone producers). The Cretaceous K37/K38 ratio is distinctly low (<0.5) and thus more like that of modern marine core-top samples and cultures of *E. huxleyi* and *G. oceanica*.

The characteristics of the Cretaceous alkenones described above conform with their ancestral position on the phylogenetic tree (Fig. 2C). Specifically, we find a general pattern of increasing K37/K38 ratio and increased variability as the lineage diverged from marine to brackish and lacustrine settings (Fig. 2C). If we accept that $C_{36:2}$Et with a C_5 double-bond spacing identified in brackish waters is produced by the more recently evolved Group II, then there appears to be a trend toward shortening the double-bond separation in $C_{36:2}$Et over time. Note that this simple linear interpretation is parsimonious and oversimplifies the complex evolutionary history of the Isochrysidales. More combined stratigraphic and geographic investigations on alkenone profiles and molecular structures are necessary to fully disentangle the evolution of the alkenone biosynthetic pathway of Isochrysidales since the Cretaceous (Rontani et al., 2006; Brassell, 2014).

One major concern raised by the evolution of the alkenone producers is that the carbon isotope fractionation of alkenones relative to the $\delta^{13}C_{DIC}$, where DIC is dissolved inorganic carbon, might be lineage specific. The mixing of alkenones produced by different algal lineages in the Black Sea, for instance, led to highly variable isotopic offsets, with carbon isotopic signatures of ~−22‰ and ~−32‰ for $C_{36:2}$Et and $C_{37:4}$Me, respectively (Freeman and Wakeham, 1992; Xu et al., 2001). Our Cretaceous samples instead show no evidence of large isotopic differences among alkenones (Table S8), which is consistent with marine Noëlaerhabdaceae in the Cenozoic. Thus, isotopic fractionation is likely conserved in marine alkenones and suitable for pCO_2 reconstructions using $\delta^{13}C$ of $C_{37:2}$Me.

In Figure 3B, we estimate that Cretaceous alkenones have an ε_p in the range of 21.6‰–26.7‰ (blue) (Table S9), which aligns with the most positive values reported in the Cenozoic (orange). Similarly, Cretaceous pCO_2 estimates of 548–4090 ppm and a median of 908 ppm are broadly within the range of Eocene pCO_2. It has long been suggested from benthic $\delta^{18}O$ records that the Eocene and Cretaceous were two of the warmest intervals over the past 150 m.y. (Fig. 3C), with nearly flat meridional temperature gradients and warm sub-Arctic SSTs as high as 10–20 °C (O'Brien et al., 2017). To maintain

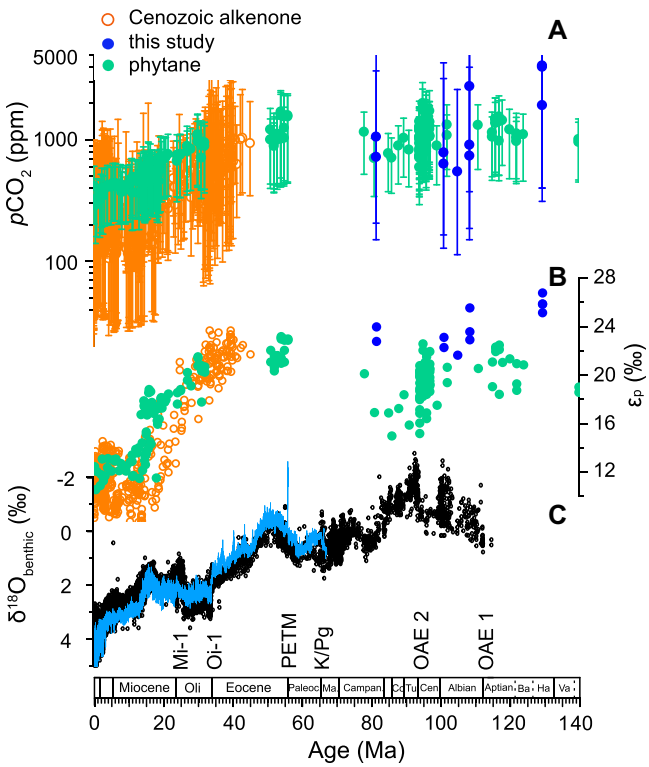

Figure 3. Cretaceous to Cenozoic pCO_2 reconstruction using organic biomarkers. (A) Published Cenozoic pCO_2 (empty circles; CENCO$_2$PIP Consortium, 2023) and new Cretaceous pCO_2 (solid circles). Error bars indicate 95% confidence interval. (B) Comparison of ε_p (carbon isotope fractionation factor) between alkenones and phytane (Witkowski et al., 2018). (C) Benthic $\delta^{18}O$ stack (blue: Westerhold et al., 2020; black: Friedrich et al., 2012). Ma—Maastrichtian; Co—Coniacian; Tu—Turonian; Cen—Cenomanian; Ba—Barremian; Ha—Hauterivian; Va—Valanginian.

such warmth, climate models require pCO_2 significantly above modern levels (Tierney et al., 2020). The Cretaceous ε_p and pCO_2 estimated here from the alkenones are thus consistent with model expectations.

Our alkenone-based estimates are also in broad agreement with phytane-based results (Fig. 3, green). This suggests that both proxies are consistent at elevated levels of CO_2 and bolsters previous efforts to estimate pCO_2 via phytane through the Phanerozoic (Witkowski et al., 2018). Because of the alkenones' specific taxonomic origin, future paired estimates of ε_p and pCO_2 via Mesozoic alkenones and phytane (or phytol) hold promise for refining phytane-based pCO_2 estimates that predate the origin of alkenones.

Our documentation of Cretaceous marine alkenones like those secreted in the coccolith-bearing family Noëlaerhabdaceae (51–0 Ma) invites us to reconsider the origin of calcification in the order Isochrysidales. Despite earlier reports of alkenones in Aptian–Cenomanian black shales (e.g., Brassell et al., 2004), the current consensus is that there is no record of calcifying marine Isochrysidales in the Cretaceous, calcification in this order being restricted to the early Eocene to present (Henderiks et al., 2022). Yet, molecular biology indicates a deep origin of the marine Isochrysidales (Medlin et al., 2008; Liu et al., 2010; Richter et al., 2019) well before 66 Ma. Consistent occurrences of alkenones from the Hauterivian through Campanian implies that unsuspected coccolith-bearing species in this order (but not in the family Noëlaerhabdaceae) synthesized alkenones already by ca. 132 Ma. The identification of Mesozoic Isochrysidales coccoliths may not be straightforward. As for other orders, the coccoliths of putative Mesozoic Isochrysidales may exhibit morphologies different from those of the Cenozoic, and diagenetic processes may complicate the recognition of morphological affinities (Aubry, 2018, 2021). However, two likely Isochrysidales candidates are the Mesozoic genera of *Repagulum* and *Pickelhaube* based on their morphostructure and reported occurrences that have guided our sampling for alkenone analysis (see the Supplemental Material). This work calls for a re-evaluation of the phylogenetic links between Mesozoic and Cenozoic coccolithophores.

SUMMARY

Alkadienones in the Atlantic Basin between ca. 80 and 130 Ma are described. These Cretaceous alkenones are characterized by a low K37/K38 ratio and by the unique occurrence of $C_{36:2}$Et, $C_{41:2}$Me, and $C_{42:2}$Et, which are not commonly seen in Cenozoic marine records. Early Cretaceous samples also reveal a novel $C_{36:2}$Et with double-bond positions separated by nine carbons. Nevertheless, the broad comparability of $\delta^{13}C$ between alkenone constituents, as observed in the Cenozoic, suggests parsimoniously a coherence in Mesozoic and Cenozoic alkenone biosynthesis. With the assumption isotopic fractionation is also conserved during the evolution of marine alkenone-producing algae, we apply a Cenozoic pCO_2 calibration to Cretaceous alkenones. The calculated ε_p reveals the most positive values over the past 130 m.y., suggesting pCO_2 in the range 548–4090 ppm (with a median of 908 ppm). These estimates align with phytane-based reconstructions, suggesting elevated pCO_2 during the hothouse climate in the Cretaceous.

ACKNOWLEDGMENTS

Si is partially supported by OCE-2202760 and RII Track-4:NSF 2327230. Aubry and Si designed the experiment; Si and Novak conducted the experiments; Richter and Si performed DMDS analysis; Si and Santos performed isotope ratio mass spectrometry analysis; Nirenberg and Novak analyzed GDGT; Polissar and Novak calculated pCO_2; Aubry and Ma discussed fossil records. All authors contributed to the writing of the manuscript. The authors thank Yongsong Huang, Simon Brassell, and Yige Zhang for constructive comments.

REFERENCES CITED

Aubry, M.-P., 2018, Peering into the biology of extinct coccolithophores: The Order Discoasterales, *in* Denne, R.A., and Kahn, A., eds., Geologic Problem Solving with Microfossils IV: SEPM (Society for Sedimentary Geology) Special Publication 111, p. 65–93, https://doi.org/10.2110/sepmsp.111.09.

Aubry, M.-P., 2021, Coccolithophores: Cenozoic Discoasterales—Biology, Taxonomy, Stratigraphy: SEPM (Society for Sedimentary Geology) Concepts in Sedimentology and Paleontology 14, 452 p., https://doi.org/10.2110/sepmcsp.14.

Brassell, S.C., 2014, Climatic influences on the Paleogene evolution of alkenones: Paleoceanography, v. 29, p. 255–272, https://doi.org/10.1002/2013PA002576.

Brassell, S.C., Dumitrescu, M., and the ODP Leg 198 Shipboard Scientific Party, 2004, Recognition of alkenones in a lower Aptian porcellanite from the west-central Pacific: Organic Geochemistry, v. 35, p. 181–188, https://doi.org/10.1016/j.orggeochem.2003.09.003.

CENCO$_2$PIP Consortium (Cenozoic CO_2 Proxy Integration Project Consortium), 2023, Toward a Cenozoic history of atmospheric CO_2: Science, v. 382, https://doi.org/10.1126/science.adi5177.

de Bar, M.W., Rampen, S.W., Hopmans, E.C., Sinninghe Damsté, J.S., and Schouten, S., 2019, Constraining the applicability of organic paleotemperature proxies for the last 90 Myrs: Organic Geochemistry, v. 128, p. 122–136, https://doi.org/10.1016/j.orggeochem.2018.12.005.

Doiron, K.E., Brassell, S.C., Bijl, P.K., Wagner, T., Herrle, J., Uenzelmann-Neben, G., Bohaty, S.M., Childress, L.B., and IODP Expedition 392 Science Party, 2023, Evolutionary lineages of alkenones recorded in Cretaceous and Paleocene sediments from the Transkei Basin (IODP Site U1581): Abstract presented at Goldschmidt 2023, Lyon, France, 9–14 July, https://doi.org/10.7185/gold2023.20482.

Dumitrescu, M., and Brassell, S.C., 2005, Biogeochemical assessment of sources of organic matter and paleoproductivity during the early Aptian Oceanic Anoxic Event at Shatsky Rise, ODP Leg 198: Organic Geochemistry, v. 36, p. 1002–1022, https://doi.org/10.1016/j.orggeochem.2005.03.001.

Foster, G.L., Royer, D.L., and Lunt, D.J., 2017, Future climate forcing potentially without precedent in the last 420 million years: Nature Communications, v. 8, https://doi.org/10.1038/ncomms14845.

Freeman, K.H., and Wakeham, S.G., 1992, Variations in the distributions and isotopic composition of alkenones in Black Sea particles and sediments: Organic Geochemistry, v. 19, p. 277–285, https://doi.org/10.1016/0146-6380(92)90043-W.

Friedrich, O., Norris, R.D., and Erbacher, J., 2012, Evolution of middle to Late Cretaceous oceans—A 55 m.y. record of Earth's temperature and carbon cycle: Geology, v. 40, p. 107–110, https://doi.org/10.1130/G32701.1.

Hasegawa, T., and Goto, A.S., 2024, Paleoceanographic importance of tri-and di-unsaturated alkenones through the early phase of Cretaceous Oceanic Anoxic Event 2 from southern high latitudes of the proto-Indian Ocean: Organic Geochemistry, v. 188, https://doi.org/10.1016/j.orggeochem.2023.104722.

Hay, W.W., and Floegel, S., 2012, New thoughts about the Cretaceous climate and oceans: Earth-Science Reviews, v. 115, p. 262–272, https://doi.org/10.1016/j.earscirev.2012.09.008.

Henderiks, J., and Pagani, M., 2008, Coccolithophore cell size and the Paleogene decline in atmospheric CO_2: Earth and Planetary Science Letters, v. 269, p. 576–584, https://doi.org/10.1016/j.epsl.2008.03.016.

Henderiks, J., Sturm, D., Šupraha, L., and Langer, G., 2022, Evolutionary rates in the Haptophyta: Exploring molecular and phenotypic diversity: Journal of Marine Science and Engineering, v. 10, 798, https://doi.org/10.3390/jmse10060798.

Huang, Y., Zheng, Y., Heng, P., Giosan, L., and Coolen, M.J.L., 2021, Black Sea paleosalinity evolution since the last deglaciation reconstructed from alkenone-inferred Isochrysidales diversity: Earth and Planetary Science Letters, v. 564, https://doi.org/10.1016/j.epsl.2021.116881.

Jagniecki, E.A., Lowenstein, T.K., Jenkins, D.M., and Demicco, R.V., 2015, Eocene atmospheric CO_2 from the nahcolite proxy: Geology, v. 43, p. 1075–1078, https://doi.org/10.1130/G36886.1.

Liao, S., Yao, Y., Wang, L., Wang, K.J., Amaral-Zettler, L., Longo, W.M., and Huang, Y., 2020, C_{41} methyl and C_{42} ethyl alkenones are biomarkers for Group II Isochrysidales: Organic Geochemistry, v. 147, https://doi.org/10.1016/j.orggeochem.2020.104081.

Liu, H., Aris-Brosou, S., Probert, I., and de Vargas, C., 2010, A time line of the environmental genetics of the haptophytes: Molecular Biology and Evolution, v. 27, p. 161–176, https://doi.org/10.1093/molbev/msp222.

Marlow, J.R., Farrimond, P., and Rosell-Melé, A., 2001, Analysis of lipid biomarkers in sediments from the Benguela Current coastal upwelling system (Site 1084), *in* Wefer, G., et al., eds., Proceedings of the Ocean Drilling Program, Scientific Results, Volume 175: College Station, Texas, Ocean Drilling Program, p. 1–26.

Marlowe, I.T., Brassell, S.C., Eglinton, G., and Green, J.C., 1990, Long-chain alkenones and alkyl alkenoates and the fossil coccolith record of marine sediments: Chemical Geology, v. 88, p. 349–375, https://doi.org/10.1016/0009-2541(90)90098-R.

Medlin, L.K., Sáez, A.G., and Young, J.R., 2008, A molecular clock for coccolithophores and implications for selectivity of phytoplankton extinctions across the K/T boundary: Marine Micropaleontology, v. 67, p. 69–86, https://doi.org/10.1016/j.marmicro.2007.08.007.

O'Brien, C.L., et al., 2017, Cretaceous sea-surface temperature evolution: Constraints from TEX_{86} and planktonic foraminiferal oxygen isotopes: Earth-Science Reviews, v. 172, p. 224–247, https://doi.org/10.1016/j.earscirev.2017.07.012.

Pearson, P.N., Ditchfield, P.W., Singano, J., Harcourt-Brown, K.G., Nicholas, C.J., Olsson, R.K., Shackleton, N.J., and Hall, M.A., 2001, Warm tropical sea surface temperatures in the Late Cretaceous and Eocene epochs: Nature, v. 413, p. 481–487, https://doi.org/10.1038/35097000.

Prahl, F.G., Rontani, J.-F., Volkman, J.K., Sparrow, M.A., and Royer, I.M., 2006, Unusual C_{35} and C_{36} alkenones in a paleoceanographic benchmark strain of *Emiliania huxleyi*: Geochimica et Cosmochimica Acta, v. 70, p. 2856–2867, https://doi.org/10.1016/j.gca.2006.03.009.

Richter, N., Longo, W.M., George, S., Shipunova, A., Huang, Y., and Amaral-Zettler, L., 2019, Phylogenetic diversity in freshwater-dwelling Isochrysidales haptophytes with implications for alkenone production: Geobiology, v. 17, p. 272–280, https://doi.org/10.1111/gbi.12330.

Rontani, J.-F., Prahl, F.G., and Volkman, J.K., 2006, Characterization of unusual alkenones and alkyl alkenoates by electron ionization gas chromatography/mass spectrometry: Rapid Communications in Mass Spectrometry, v. 20, p. 583–588, https://doi.org/10.1002/rcm.2346.

Stoll, H.M., Guitian, J., Hernandez-Almeida, I., Mejia, L.M., Phelps, S., Polissar, P., Rosenthal, Y., Zhang, H., and Ziveri, P., 2019, Upregulation of phytoplankton carbon concentrating mechanisms during low CO_2 glacial periods and implications for the phytoplankton pCO_2 proxy: Quaternary Science Reviews, v. 208, p. 1–20, https://doi.org/10.1016/j.quascirev.2019.01.012.

Tierney, J.E., et al., 2020, Past climates inform our future: Science, v. 370, https://doi.org/10.1126/science.aay3701.

Westerhold, T., et al., 2020, An astronomically dated record of Earth's climate and its predictability over the last 66 million years: Science, v. 369, p. 1383–1387, https://doi.org/10.1126/science.aba6853.

Witkowski, C.R., Weijers, J.W., Blais, B., Schouten, S., and Sinninghe Damsté, J.S., 2018, Molecular fossils from phytoplankton reveal secular pCO_2 trend over the Phanerozoic: Science Advances, v. 4, https://doi.org/10.1126/sciadv.aat4556.

Xu, L., Reddy, C.M., Farrington, J.W., Frysinger, G.S., Gaines, R.B., Johnson, C.G., Nelson, R.K., and Eglinton, T.I., 2001, Identification of a novel alkenone in Black Sea sediments: Organic Geochemistry, v. 32, p. 633–645, https://doi.org/10.1016/S0146-6380(01)00019-5.

Yamamoto, M., Ficken, K., Baas, M., Bosch, H.-J., and de Leeuw, J.W., 1996, Molecular palaeontology of the earliest Danian at Geulhemmerberg (the Netherlands): Netherlands Journal of Geosciences, v. 75, p. 255–267.

Zhang, Y.G., Pagani, M., Liu, Z., Bohaty, S.M., and DeConto, R., 2013, A 40-million-year history of atmospheric CO_2: Philosophical Transactions of the Royal Society of London: Series A, Mathematical, Physical, and Engineering Sciences, v. 371, https://doi.org/10.1098/rsta.2013.0096.

Zheng, Y., Dillon, J.T., Zhang, Y., and Huang, Y., 2016, Discovery of alkenones with variable methylene-interrupted double bonds: Implications for the biosynthetic pathway: Journal of Phycology, v. 52, p. 1037–1050, https://doi.org/10.1111/jpy.12461.

Printed in the USA